

## AEROGEL TRACK MORPHOLOGY: MEASUREMENT, THREE DIMENSIONAL RECONSTRUCTION AND PARTICLE LOCATION USING CONFOCAL LASER SCANNING MICROSCOPY.

A.T. Kearsley<sup>1</sup>, A.D. Ball<sup>1</sup>, G.A. Graham<sup>2</sup>, M.J. Burchell<sup>3</sup>, H. Ishii<sup>2</sup>, M.J. Cole<sup>3</sup>, P.A. Wozniakiewicz<sup>1</sup>, F. Hörz<sup>4</sup> and T.H. See<sup>4</sup>.  
<sup>1</sup>Department of Mineralogy, Natural History Museum, London, SW7 5BD, UK, ([antk@nhm.ac.uk](mailto:antk@nhm.ac.uk)), <sup>2</sup>Institute of Geophysics and Planetary Physics, Lawrence Livermore National Laboratory, 7000 East Avenue, Livermore, CA 94550-9234, USA, <sup>3</sup>Centre for Astrophysics and Planetary Sciences, School of Physical Science, University of Kent, Canterbury, CT2 7NR, UK, <sup>4</sup>NASA Johnson Space Centre, Houston, Texas, USA.

**Introduction:** The Stardust spacecraft returned the first undoubted samples of cometary dust, with many grains embedded in the silica aerogel collector [1,2]. Although many tracks contain one or more large terminal particles of a wide range of mineral compositions [3], there is also abundant material along the track walls [4]. To help interpret the full particle size, structure and mass, both experimental simulation of impact by shots [5] and numerical modeling of the impact process [6] have been attempted. However, all approaches require accurate and precise measurement of impact track size parameters such as length, width and volume of specific portions. To make such measurements is not easy, especially if extensive aerogel fracturing and discoloration has occurred. In this paper we describe the application and limitations of laser confocal imagery for determination of aerogel track parameters, and for the location of particle remains.

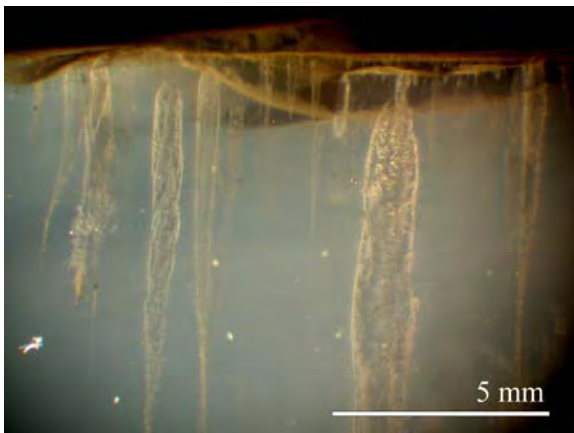


Figure 1. Incident light images of tracks formed by impact of basalt glass grains at  $6 \text{ km s}^{-1}$  into  $60 \text{ kg m}^{-3}$  silica aerogel, note complex track structure.

**Experimental Analogues:** We used aerogel targets from buckshot firings with the two-stage light gas gun (LGG) at the University of Kent, Canterbury [7] using the same basalt glass projectiles as [8].

**Instrumental Techniques:** A wide variety of imaging and analytical techniques have been applied to aerogel tracks [9]. Particular success has been achieved in location of higher-density compacted

aerogel and residue debris by X-ray ultramicroscopy (XuM) [10], scanning transmission ion microscopy (STIM) [11] and synchrotron X-ray fluorescence analysis (SXRF) [4]. However, XuM does not directly yield compositional information, and both SXRF and STIM require extraction of the track into a relatively small subsample before imaging, although they also provide microanalyses. The good optical transmission properties of aerogel have allowed use of laser Raman microscopy to locate and characterise organic and mineral particles in laboratory experiments [12,13,14,15]. Another laser-based technique, confocal laser scanning microscopy (CLSM), has a remarkable pedigree in many biological applications, where the excellent depth resolution ( $< 500 \text{ nm}$ ) allows detailed imaging of transparent samples such as cell organelles [16], especially by use of fluorescent labelling. Two-dimensional digital depth slice images created by CLSM can be assembled as three-dimensional models, from which feature sizes and volumes can be calculated.



Figure 2. The Leica TCS NT Confocal laser scanning microscope at the Natural History Museum, London.

The Leica TCS NT is based on a DMR upright transmitted and reflected light microscope. For confocal imaging, three lasers are used: Ar (476 and 488nm), Kr (568nm), He-Ne (633nm), with tunable detection bands. The software allows simultaneous or sequential scanning of three fluorescence/reflectance channels and one transmitted light channel. Single X-

Y slices can be captured, or Z-axis stacks of slices to provide volumetric measurements and rendered 3D images. Spatial resolution depends on the objective lens and aperture, e.g. a 10x objective and n.a. 3 aperture give a 1mm X-axis field of view, Z-axis stack interval of 2.4 $\mu$ m and 1.95x1.95x2.4 $\mu$ m voxel (volume element) size.

**Results:** We have obtained CLSM depth slice stacks from laser reflectance of hypervelocity impact tracks and embedded projectile grains in silica aerogel of a wide range of density ( $\sim 5 - 60 \text{ kg m}^{-3}$ ), both in large (3cm) blocks and sub-millimetre keystones [17]. The main mass of the aerogel gives a little laser scattering background, as expected from the ‘blue smoke’ appearance characteristic of silica aerogel. The track edges are accentuated by strong contrast between a zone of intense laser scattering in dense aerogel and absence of reflected signal from the empty track.

Red ( $\lambda$  612-648 nm) and blue-green ( $\lambda$  472-508nm) scattering is strongest from fractured and dense aerogel at track margins, around terminal particles and on rough-cut keystone surfaces. Yellow ( $\lambda$  556-582 nm) reflection is particularly strong from basalt glass fragments, and the larger particles correspond to the dark grains seen in our optical images.

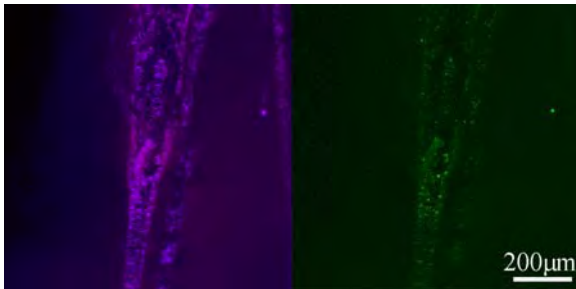


Figure 3. Tracks, in CLSM, all depth slices combined (equivalent to full-thickness image). Red and blue-green reflections combined at left, yellow at right.

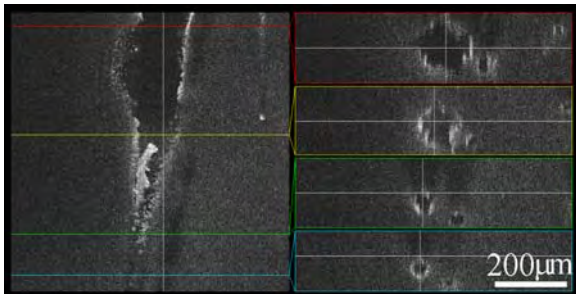


Figure 4. A track in aerogel seen in combined red and blue-green reflection images; left, a single depth slice; right, four cross sections from the lines indicated.

In Fig 4, a single CLSM slice (left) shows sections through two tracks at this level. The large track at left has a ‘carrot’ form [2] common to impacts by solid particles of relatively high density [5]. A large radial fracture is visible as a sub-circular protrusion to the left of the main track. The cross sections (right) reveal complex shape for the upper part of the large track, and also a further two tracks (arrowed) whose width can be measured.

**Conclusions:** CLSM should prove to be a valuable technique for quantification of aerogel track morphology and particle location, especially for the small tracks expected in aerogel on the interstellar side of the Stardust Sample Tray Assembly. CLSM can be performed on samples in aerogel keystones or quickstones [18], and also on cm-scale, unprepared aerogel blocks. It is therefore suitable for track characterisation at an early stage of curation and preparation. Selection of precise wavelengths for image collection is critical to success in distinguishing particle residue from dense aerogel, although reflections across a wide  $\lambda$  range can reveal the aerogel surface, permitting imaging of the track morphology.

**References:** [1] Brownlee D.E. et al. (2006) *Science*, 314, 1711-1716. [2] Hörz F. et al. (2006) *Science*, 314, 1716-1719. [3] Zolensky M.E. et al. (2006) *Science*, 314, 1735-1739. [4] Flynn G. et al. (2006) *Science*, 314, 1731-1735. [5] Burchell M.J. et al. Characteristics of cometary dust tracks in Stardust aerogel and laboratory calibrations, submitted to *MAPS*. [6] Domínguez G. et al. (2004) *Icarus* 172, 613-624. [7] Burchell M.J. et al. (1999) *Meas. Sci. Tech.* 10, 41-50. [8] Kearsley A.T. et al. (2007) *MAPS*, 42.2, in press. [9] Burchell M.J. et al. (2006) *Ann. Rev. Earth Planet. Sci.*, 34, 385-418. [10] Graham G.A. et al. (2005) *LPSC XXXVI*, #2078. [11] Graham G.A. et al. (2004) *MAPS*, 39.9, 1461-1473. [12] Burchell M.J. et al. (2001) *MAPS*, 36, 209-221. [13] Graham G.A. et al. (2001) *Proc. Roy. Microscopical Soc.*, 36/4, 251-254. [14] Burchell M.J. et al. (2004) *J. Raman Spectr.*, 35, 249-253. [15] Burchell M.J. et al. (2006) *MAPS*, 41.2, 217-232. [16] <http://www.olympusconfocal.com/theory/> [17] Westphal A. et al. *MAPS*, 39, 1375-86. [18] Ishii H.A. et al. (2005) *MAPS*, 40.11, 1755-1759.

**Acknowledgements:** We thank NASA for the Stardust aerogel block used as target in the basalt powder shot; PPARC for support of the gun facility at Canterbury; Andrew Westphal and Chris Snead at Berkeley for preparation of the keystone. Staff at LLNL acknowledge their work was performed under the auspices of the US Department of Energy by the Lawrence Livermore National Laboratory under Contract No. W-7405-ENG-48.